Excitation Energy Transfer from Carotenoid to Bacteriochlorophyll in the Photosynthetic Purple Bacterial Reaction Center of *Rhodobacter sphaeroides*

Su Lin,* Evaldas Katilius, Aileen K. W. Taguchi, and Neal W. Woodbury

Department of Chemistry and Biochemistry and the Center for the Study of Early Events in Photosynthesis, Arizona State University, Tempe, Arizona 85287-1604

Received: July 21, 2003; In Final Form: October 10, 2003

The role of carotenoid in singlet excitation energy transfer in the purple bacterial reaction center of *Rb. sphaeroides* has been studied using femtosecond transient absorbance spectroscopy techniques at room temperature. The carotenoid S_0-to-S_2 transition band was directly excited at 490 nm and the transient spectral changes were recorded in the visible and near-infrared spectral regions with subpicosecond time resolution. This result was compared with transient spectral changes observed following direct excitation of the bacteriochlorophyll dimer of the reaction center (P) at 860 nm. With 490-nm excitation, a subpicosend relaxation process from the carotenoid S_2-to-S_1 state is observed, followed by energy transfer to the monomer bacteriochlorophylls. Excitation energy is further transferred to P and then is utilized for the formation of the charge separated state $P^+H_A^-$. The majority of the excitation energy from the carotenoid is transferred to bacteriochlorophyll from its S_1 state and occurs with a time constant of 2.2 ps. The overall energy transfer efficiency between the excited carotenoid and bacteriochlorophyll is estimated to be greater than or equal to 75%. The carotenoid in the purple bacterial reaction center is in a 15-cis-configuration, which differs from the all-trans configuration of carotenoids found in the vast majority of antenna systems. The efficient singlet excitation energy transfer observed in this study suggests that the configuration difference is not a key factor in determining the efficiency of carotenoid-to-bacteriochlorophyll singlet excitation energy transfer.

Introduction

Carotenoid is a key component in the light harvesting complexes and reaction centers of photosynthetic organisms. Its primary roles in photosynthesis are light harvesting and photoprotection (for review, see ref 1). Carotenoid absorbs in the visible region (420−550 nm) where the majority of photosynthetic pigments, such as chlorophylls and bacteriochlorophylls (Bchl), have low extinction coefficients.[1] In photosynthetic antenna systems, the energy transfer efficiency from carotenoid to other pigments varies from 25 to ∼100%, largely depending on the structure of the individual system.[2] Carotenoids also play a role in photoprotection by dissipating excess energy. They quench the (B)chl triplet state to prevent its reaction with molecular oxygen, or react directly with singlet oxygen to detoxify it.[3−7]

The role of carotenoids in singlet−singlet excitation energy transfer in various photosynthetic antenna systems has been extensively studied. Carotenoid molecules exist in an all-trans configuration in all known antenna systems except for the photosystem I core antenna in which 5 out of 22 β-carotenes are in a cis-configuration.[8] Because the carotenoid all-trans-configuration has a C_{2h} symmetric arrangement, the one-photon S_0 ($1A_g^-$)-to-S_1 ($2A_g^-$) transition is optically forbidden. The observed carotenoid absorption band in the 420−550-nm region is due to the transition from the ground state to the second excited singlet state (S_0 ($1A_g^-$) → S_2 ($1B_u^+$)). Multiple pathways have been found for energy transfer from carotenoid to (B)chls in antenna systems, such as from the carotenoid S_2 excited state to either the Q_X or Q_Y states of (B)chls, and from the carotenoid S_1 excited state to the (B)chl Q_Y state. Due to the nature of efficient and rapid energy transfer processes involving carotenoids, ultrafast laser spectroscopic techniques play a major role in the study of singlet excited-state kinetics, using one-photon or two-photon excitation.[9−20] The excited S_2 state decays to the S_1 state within 200 fs via internal conversion.[9] The S_1 state lifetime of most carotenoids in vitro is also short, around 10 ps,[2,21] although some are found to live up to 100 ps.[10] Thus, singlet excitation energy transfer from carotenoid to other molecules must occur in most cases on the subpicosecond to picosecond time scale to compete with other decay pathways.

There is only one carotenoid in reaction centers of purple bacteria and photosystem II from green plants and algae.[22] The reaction center of *Rb. sphaeroides* contains one noncovalently bound spheroidene molecule (or spheroidenone molecule, depending on the growth conditions[3,5,23]), which, unlike antenna cartenoids, is present in a 15-cis-configuration.[24,25] In addition to the carotenoid, the reaction center contains four bacteriochlorophylls, two bacteriopheophytins and two quinones arranged in a roughly symmetric fashion about a C_2 axis (Figure 1). A pair of Bchls, P (the initial electron donor) sits near the periplasmic side of the complex. To either side of P are two monomer Bchls (B_A and B_B), then two bacteriopheophytins (H_A and H_B), and finally two quinones (Q_A and Q_B) near the cytoplasmic side of the complex. The cartonenoid is located next to B_B on the side of this cofactor opposite from P.[25,26] The structural differences between carotenoids in antenna and in reaction centers have led to the speculation that the major role of carotenoids in antenna systems is light harvesting, while the 15-cis-geometry of the carotenoid in reaction centers is optimized for quenching P triplet states.[27,28] However, the location and spectral properties of the carotenoid in reaction centers

* Author to whom correspondence should be addressed. slin@asu.edu.

10.1021/jp036130m CCC: $25.00
Published on Web 11/22/2003

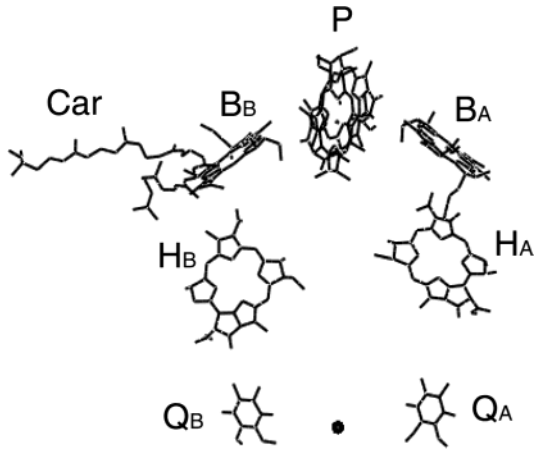

Figure 1. Arrangement of the cofactors of the photosynthetic reaction center from *Rb. sphaeroides* (from PDB entry 1A1J).

strongly suggests the possibility of light harvesting in this complex as well. In fact, it has been proposed that excitation can be transferred from carotenoid to the special pair via B_B.[29] The role carotenoid plays in singlet energy transfer in reaction centers has not been explored in detail thus far. In the cis-configuration, the carotenoid C_{2h} symmetric arrangement is broken; the energy transfer mechanisms can differ from that of all-trans carotenoids. However, absorption spectra of locked-15,15′-*cis*-spheroidene both in solution and reconstituted into the R-26 (carotenoidless) reaction center show no sign of the S_1 absorption band.[24] An earlier study by Cogdell et al. used steady-state spectroscopic techniques to measure the energy transfer from carotenoid to Bchl in purple bacterial reaction centers.[30] The efficiency of singlet excited-state energy transfer from carotenoid to P was estimated to be close to 80%.

The goal of the current study is to explore the spectroscopic and kinetic properties of the carotenoid in the bacterial reaction center with ultrafast laser spectroscopy and to obtain a better understanding of the carotenoid function in singlet state energy transfer. Wild-type reaction centers from *Rb. sphaeroides* are excited in the carotenoid absorption band at 490 nm, and absorption change spectra are monitored over a broad wavelength region from 480 to 980 nm. Rapid singlet excited-state energy transfer from the carotenoid to other reaction center cofactors is observed.

Materials and Methods

Procedures for preparation of wild-type reaction centers of *Rb. sphaeroides* have been described previously.[31] Cells were grown aerobically in the dark. Under such growth conditions, the majority of the reaction centers contain spheroidenone.[3,5,23] Reaction centers were suspended in a buffer solution of 50 mM Tris-HCl (pH 8.0), 0.025% LDAO, 1 mM EDTA, and 0.1 mM orthophenanthroline. For femtosecond transient spectral measurements, samples were loaded into a spinning wheel with an optical path length of 2.5 mm. An optical density of roughly 1 at 802 nm was used. All measurements were performed at room temperature.

The femtosecond transient absorption spectrometer has been described previously.[32] Laser pulses of 100 fs at 790 nm were generated from an amplified, mode-locked Titanium Sapphire kilohertz laser system (CPA-1000, Clark-MXR). Part of the laser pulse energy (~15%) was used to generate a white light continuum for probe beams. The remainder of the pulse energy was used to pump a modified optical parametric amplifier (IR-OPA, Clark-MXR) to generate excitation pulses at 490 or 860 nm. The excitation intensity was adjusted using a continuously varied neutral density filter. Transient absorption changes were measured over two spectral ranges from 460 to 760 nm and from 730 to 1030 nm with a dual diode array detector (DPDA, Princeton Instruments). The relative polarization of the excitation and probe beams was set at the magic angle. Time-resolved spectra were recorded every 91 fs with a spectral resolution of 2 nm. The energy per pulse was kept below 2 μJ with a spot size of 1-mm diameter to avoid multiple photon excitation of reaction centers.

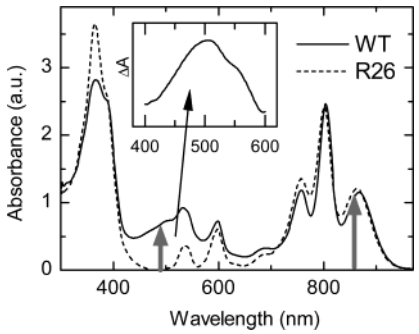

Figure 2. Absorption spectra of wild-type (solid line) and R-26 (dashed line) reaction centers at room temperature. Spectra were recorded with 1-nm resolution and normalized at the B band Q_Y transition peak wavelength (802 nm). The gray arrows indicate excitation wavelengths at 490 and 860 nm. The inset shows the difference spectrum of the two types of reaction centers.

Time-resolved spectra were corrected for spectral dispersion. Data analysis was carried out using locally written software (ASUFIT) developed under a MatLab environment.

Results and Discussion

The Ground-State Absorbance Spectrum of the Reaction Center Carotenoid. Steady-state absorption spectra of wild-type and R-26 reaction centers from *Rb. sphaeroides* recorded at 298 K are shown in Figure 2. The two spectra were normalized at 802 nm. The major structural difference between wild-type and R-26 reaction centers is that the latter does not contain any carotenoid. This difference results in less absorption in the 500-nm region. The inset in Figure 2 shows the spectral difference between the two reaction centers, obtained by subtracting the R-26 absorption spectrum from the spectrum of wild-type reaction centers. The spectral difference between the two types of reaction centers indicates that carotenoid in wild-type reaction centers makes a major contribution to the absorption around 500 nm. Transient absorbance changes in wild-type reaction centers in this study were recorded with excitation at 490 nm, which preferentially excites the carotenoid S_0-to-S_2 transition. Data from 860-nm excitation were also collected as a reference. The thick gray arrows in Figure 2 indicate the wavelengths used for excitation (490 and 860 nm).

Formation and Decay of Carotenoid Excited States. Transient absorption changes between 500 and 700 nm with 490-nm excitation are plotted in Figure 3. The absorbance difference spectra in Figure 3a illustrate the early time spectral evolution of the carotenoid excited state in reaction centers. Spectral changes at 0 ps show a broad bleaching of the band centered around 500 nm, which represents a prompt bleaching of the carotenoid ground state due to formation of the S_2 excited state. A broad absorbance increase rapidly grows in on the long wavelength side. The 500-nm bleaching reaches its maximum between 300 and 400 fs, while the absorption increase around 600 nm is not fully developed until 600 fs. A weak bleaching

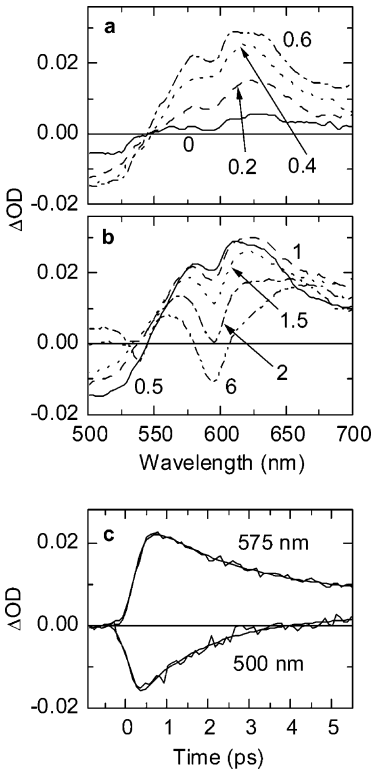

Figure 3. Transient absorbance change spectra of wild-type reaction centers with 490-nm excitation, recorded (a) from 0 to 0.6 ps and (b) from 0.5 to 6 ps. (c) Kinetics at 500 and 575 nm fit by a multiple exponential decay (smooth curves, see text for the fitting parameters).

at 595 nm superimposed on top of the excited-state absorption can be seen clearly in the 0.6-ps spectrum, and this is due to the ground-state bleaching of P or B.

Previous transient absorption measurements on various systems containing carotenoids have shown that the spectral changes induced by carotenoid excited states have many features in common, including a prompt ground-state bleaching/stimulated emission at wavelengths shorter than 580 nm due to the S_0-to-S_2 transition, and a fast relaxation from the S_2 to S_1 state, resulting in an S_1-to-S_N excited-state absorption between 510 and 700 nm during the S_1 lifetime.[20,24,33−35] The transient absorption spectra shown in Figure 3a are generally consistent with those observations. The S_1-to-S_N transition shows a broad absorption increase peaking near 610 nm, and this band resembles the spectral features of all-trans spheroidenone in LH2 (Polivka, unpublished data). This suggests that the optical properties of 15-*cis*-spheroidenone in the reaction center are similar to those of *all-trans*-carotenoids in solution and in antenna systems. In addition, the 200−300-fs relaxation process from the carotenoid S_2-to-S_1 state agrees well with previous measurements by other groups of the excited-state kinetics of isolated carotenoid and of carotenoid in antenna systems.[9,10,36]

Spectral changes between 0.5 and 6 ps are shown in Figure 3b. The carotenoid ground-state bleaching fully recovers during this time period, as does the excited-state absorbance in the 550−650-nm region. The 595-nm bleaching becomes progressively more pronounced on the picosecond time scale as does a bleaching at 545 nm, though the 545-nm bleaching lags somewhat behind the growth of the 595-nm bleaching, and does not reach its maximal depth until roughly 10 ps. An absorption increase centered at 665 nm accompanies the development of the 545-nm bleaching. At 6 ps, the time-resolved spectra with either 490 or 860 nm excitation are essentially the same (860-nm data not shown). The spectrum at 6 ps in Figure 3b is also very similar to the spectrum of the charge-separated state $P^+H_A^-$.[37] The 595-nm bleaching is due to P* or B* formation initially and P^+ formation on a longer time scale. The 545-nm bleaching and 665-nm absorbance increase are due to formation of the H_A anion. The fact that the carotenoid excited-state signals are maximal before the 595-nm (bacteriochlorophyll) bleaching has completely developed and that the 595-nm bleaching occurs on a faster time scale than absorbance changes due to H_A^- formation suggests that the majority of the Bchl excitation energy used for $P^+H_A^-$ formation comes via energy transfer from the excited carotenoid to Bchl.

Kinetic traces at 500 and 575 nm with fits derived from a global fit of the time vs wavelength absorbance change surface (all wavelengths fit simultaneously) using a multiexponential function are plotted in Figure 3c. As shown, the bleaching at 500 nm recovers almost completely with a time constant of 1.6 $\pm$ 0.1 ps. The kinetics at 575 nm differs from that at 500 nm in that a rise component of 0.25 $\pm$ 0.05 ps is needed. This is consistent with the qualitative conclusion stated above that the formation of the S_1 excited-state absorbance lags behind the ground-state bleaching at 500 nm; this lag is presumably due to the S_2-to-S_1 relaxation. A 1.6-ps decay component is also found in the 575-nm trace, as is a nondecaying component. The 1.6 ps overall lifetime of the carotenoid S_1 excited state is considerably shorter than that observed for isolated spheroidenone in solution (6 $\pm$ 1 ps).[38] This fact, combined with the development of the Bchl ground-state bleaching on the same time scale, suggests that a substantial amount of excitation energy from the carotenoid is transferred to reaction center Bchls.

Energy Transfer from Carotenoid to Bchls. To further characterize the energy transfer from carotenoid to Bchl, a detailed kinetic analysis of the 595-nm band (ground-state bleaching of the bacteriochlorophylls) was performed. Figure 4a illustrates a set of absorbance change spectra around 595 nm at several representative delays following 490-nm excitation. The development of the 595-nm band is correlated with the decay of the broad carotenoid S_1 excited-state absorption in this spectral region. A straight line connecting the peaks on both sides of the 595-nm bleaching is added to approximate the background from carotenoid excited-state absorbance and to provide a better means of estimating the size of the Bchl ground-state bleaching. Figure 4b shows the same set of spectra as in Figure 4a after the excited-state absorption background has been removed. This clearly shows that the majority of the excited/charge-separated states involving B and P are not formed promptly by laser excitation. The amplitude of the 595-nm bleaching from Figure 4b was plotted as a function of the delay time in Figure 4c. The curve can be fit with a single-exponential decay of 1.5 $\pm$ 0.1 ps. This number is in excellent agreement with the recovery time of the carotenoid excited state (Figure 3c), which again suggests excitation energy transfer from carotenoid to bacteriochlorophyll. It is estimated from Figure 4c that at 0.5 ps when the carotenoid S_1 state reaches its maximum, about 30% of the P/B band at 595 nm has already developed. As only 20% of the bleaching should be formed at this time delay with the formation time of 1.5 ps, the other 10% is likely due to a combination of rapid energy transfer from carotenoid to B or P, induced absorbance changes of B_B due to its orbital overlap with carotenoid,[39] and/or some direct excitation of B or P. Similar observations were also found in the Bchl Q_Y transition region (see below).

Spectral changes in the Bchl Q_Y transition region between 750 and 950 nm comparing 490- with 860-nm excitation are

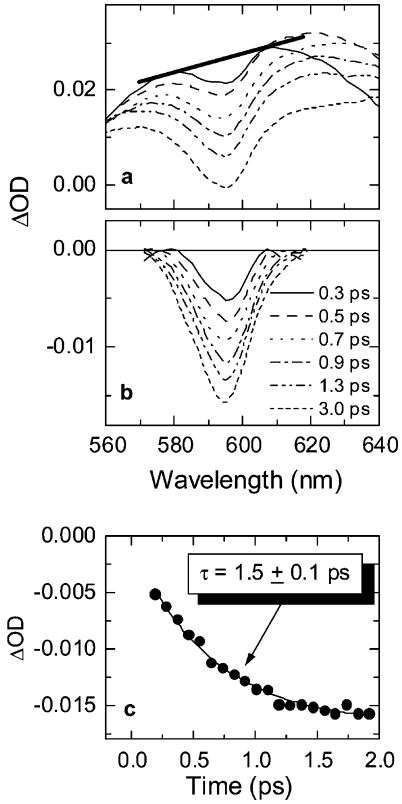

Figure 4. Absorbance change spectra of the 595-nm bleaching band with 490-nm excitation. (a) Time-resolved spectra recorded at various delay times and (b) background-corrected time-resolved spectra from (a), as obtained after subtraction of the broad absorption increase that underlies the 595-nm bleaching band. (c) Amplitude of the 595-nm bleaching band as a function of time. The curve was fit with a single-exponential decay and an offset.

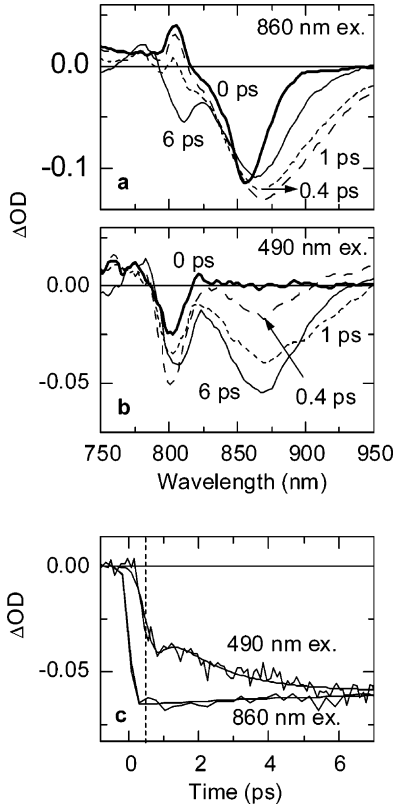

Figure 5. Comparison of time-resolved spectral changes in the Q_Y transition region with (a) 860- and (b) 490-nm excitation. Time zero is defined as the delay when about 80% of the bleaching at 860 nm with 860-nm excitation (or about 50% of the bleaching at 800 nm with 490-nm excitation) has developed. It should be pointed out that the time zero in (b) may not line up accurately with the time zero defined in Figure 3a due to the difference of optics sets used in the measurement and the lack of carotenoid signal in the near-IR region. (c) Comparison of the kinetics at 840 nm with 490- and 860-nm excitation.

shown in Figure 5. The spectral changes with 860-nm excitation exhibit a simple kinetic behavior. The initial spectral changes are dominated by the formation of P* featuring a broad bleaching of the ground-state band of P peaking at 860 nm and stimulated emission from P* at longer wavelengths (Figure 5a). The changes due to the decay of P* and formation of $P^+H_A^-$ can be seen over the subsequent 6 ps (the normal time constant for electron transfer from P* forming $P^+H_A^-$ is about 3 ps[40]). Over this time period, one observes the recovery of the stimulated emission from P* near 900 nm and the appearance of a derivative-shaped absorbance change in the 780−810-nm region associated with the electrochromic shift of one or both monomer bacteriochlorophylls.

In contrast, excitation at 490 nm initially induces an absorption decrease of the B band around 802 nm and a broad absorption increase below 800 nm (Figure 5a, 0 ps spectrum), but no bleaching of P. Time-resolved spectra at later times show partial recovery of the B band mostly within 1 ps and development of the P band at 860 nm within the first 6 ps. The spectrum at 6 ps shows the signature of the $P^+H_A^-$ state, similar to that with 860-nm excitation, though some of the 802-nm bleaching remains. The delay in formation of P bleaching is consistent with a picosecond time scale energy transfer from the carotenoid S_1 state to P (probably via B, but this cannot be resolved due to the fact that the B*-to-P* energy transfer occurs on the hundreds of femtoseconds time scale and is therefore faster than the 1.6-ps energy transfer from carotenoid to P). The prompt buildup of B* could originate from direct excitation of B, from absorbance changes in the B ground-state band induced by mixing of carotenoid and B_B orbitals,[39] or from ultrafast energy transfer between the carotenoid S_2 state and B, followed by ultrafast energy transfer to P. As both direct excitation of B and energy transfer from the carotenoid S_2 state to B occur on the time scale of the excitation pulse duration, it is difficult to differentiate one from the other.

Kinetic traces at 840 nm with excitation at 490 and 860 nm are compared in Figure 5c. The kinetics at this wavelength almost exclusively represents the ground-state bleaching of P. The two curves are normalized to the final amount of P^+ formed at times longer than 10 ps. The 860-nm excitation induced a prompt bleaching at 840 nm due to the formation of P* initially and P^+ at later times. The amplitude of the 840-nm bleaching stays essentially constant once it is formed. In contrast, a biphasic development of the bleaching signal is observed with 490-nm excitation. About 40% of this total bleaching occurs within 0.5 ps (Figure 5c). This can be understood in terms of the various ways of forming B* upon 490-nm excitation, which is then followed by rapid (100−200 fs) energy transfer to P.[41−44] First, about 20% of the 1.6 ps energy transfer from the S_1 state of the carotenoid to B has taken place by 0.5 ps, as calculated in the Q_X region. An additional 20% of B* is rapidly formed either due to direct excitation or due to energy transfer from the carotenoid S_2 state as described above. This differs slightly from the analysis described for the Q_X region above, in that case only 30% of the bleaching at 595 nm (P and B) appeared in the first 0.5 ps rather than 40%. This discrepancy is likely caused simply by the error in defining the time zero between the two spectral regions (Q_X and Q_Y). Nevertheless, the kinetics

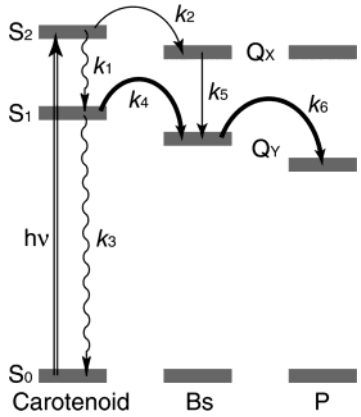

Figure 6. Proposed singlet excitation energy transfer pathways in wild-type purple bacterial reaction centers when carotenoid is excited directly.

of B or P bleaching in both the Q_X and Q_Y transition regions clearly show a biphasic rise, dominated by a 1.6-ps component due to the carotenoid-to-Bchl energy transfer.

Though this is the first time-resolved measurement of singlet energy transfer from the carotenoid to P in the reaction center, triplet energy transfer from P to the carotenoid has been studied previously.[29,39,45] By using reaction centers in which B_B has been replaced with a spectrally distinguishable cofactor, the role of B_B in triplet energy transfer from P to the carotenoid has been determined, i.e., $^3P \rightarrow {}^3B_B \rightarrow {}^3Car$, most likely via a Dexter exchange mechanism. Unfortunately, the excited monomer bacteriochlorophyll involved in the singlet energy transfer reactions described above is not well enough resolved spectrally to determine whether B_A or B_B or both serve as energy transfer intermediates. However, the location of B_B in close proximity to the carotenoid (5−6 Å) provides a likely pathway for singlet energy transfer involving the same set of molecules as suggested previously for triplet energy transfer, i.e., $^1Car \rightarrow {}^1B_B \rightarrow {}^1P$.

It is also worth mentioning that no 530/545-nm bleaching is observed at early times (<2 ps) when 490-nm excitation is used, implying that 490-nm excitation does not directly generate excited or charge separated states involving bacteriopheophytin.

Energy Transfer Efficiency. Carotenoid energy transfer efficiency in various antenna systems has been shown to vary from 25 to 100% depending largely on the structure and geometric arrangement of the pigments.[19,46] It has been rationalized that the energy transfer efficiency from the carotenoid S_1 state to the Bchl Q_Y state depends mainly on the degree of symmetry of the carotenoid and the spectral overlap between the carotenoid and (B)chl.[47] The singlet energy transfer efficiency from carotenoid to P, likely through bacteriochlorophyll monomer(s) in the purple bacterial reaction center, was estimated to be close to 80% with use of steady-state fluorescence spectroscopy.[30] This seems surprising given the fact that the carotenoid found in the bacterial reaction center is 15-cis rather than all-trans, as is found in the antenna. However, a biphasic carotenoid S_1 state decay was observed in a recent study of the photosystem I core of *Synechococuus elongatus*,[48] in which multiple isomers (including all-trans- and cis-isomers) of β-carotene exist. It was speculated that the β-carotenes in the cis-configuration are responsible for the efficient carotenoid-to-chlorophyll energy transfer (3 ps) due to a favorable $\pi-\pi$ stacking with nearby chlorophylls. The femtosecond transient absorbance measurements described here suggest that energy transfer from carotenoid to bacteriochlorophyll also occurs efficiently in the *Rb. spearoides* reaction center.

An energy transfer diagram for purple bacterial reaction centers is proposed in Figure 6 and the various rate constants associated with the energy transfer reactions are defined (k_1-k_6). Excitation at 490 nm results in the carotenoid S_0-to-S_2 transition, followed by relaxation of the excited state to S_1. The relaxation from S_2 to S_1 takes place in less than 300 fs, i.e., $k_1 \geq (0.3\ \text{ps})^{-1}$. The bulk of the bleaching of the bacteriochlorophyll ground-state absorbance at 595 nm develops with a time constant of 1.6 ps (Figure 4 and 5). This implies that the energy transfer from the carotenoid S_2 state to the Q_X state of B or P is slower than the S_2-to-S_1 relaxation. The 1.6-ps lifetime of the carotenoid ground-state bleaching near 500 nm and the coordinated decay time of the S_1-to-S_N excited-state absorption between 550 and 700 nm (Figure 3b and c) suggest that $k_3 + k_4 = (1.6\ \text{ps})^{-1}$. The intrinsic excited-state lifetime of spheroidenone in solution was measured to be 6 ± 1 ps.[38] Assuming that the intrinsic decay rate of the 15-*cis*-spheroidenone is the same in reaction centers as it is in solution, then the energy transfer rate from the carotenoid S_1 excited state to B is $k_4 = (1.6\ \text{ps})^{-1} - (6\ \text{ps})^{-1} = (2.2\ \text{ps})^{-1}$. The efficiency ($\Phi$) of energy transfer from the carotenoid S_1 state to Bchl in the reaction center is then obtained from eq 1 to be approximately 75%.

$$\Phi = \frac{k_4}{k_3 + k_4} \tag{1}$$

This estimation does not include any contribution to the energy transfer yield from the carotenoid S_2 state to B. It is shown above that about 10−20% of B bleaching is formed within the time frame of excitation pulse, and part of that could be due to ultrafast excitation transfer from the carotenoid S_2 state. It is also worth noting that the carotenoid S_1 intrinsic lifetime of 6 ps (k_3) is adapted from the lifetime measured in solution. When carotenoid is in the protein environment, the intrinsic lifetime could become longer due to the restriction of motion, vibration, and torsion, though previous S_1 lifetime measurements of β-carotene in solvents with different viscosities have shown that the S_1 decay time does not change appreciably with the environment.[49] In addition, carotenoid S_1 lifetimes in some of the bacterial antenna complexes (LH1 and LH2) have been compared to the same molecules in solution, showing essentially no change in lifetime when there is no energy transfer from the carotenoid S_1 state to bacteriochlorophyll.[17,50] In any case, corrections associated with either ignoring energy transfer from S_2 or the uncertainty in the true intrinsic lifetime of S_1 would likely result in an increased estimate for the energy transfer efficiency from excited carotenoid to bacteriochlorophyll in the reaction center. Thus, the value of 75% calculated above should be considered a lower limit. This high efficiency of energy transfer is consistent with the 80% value obtained from steady-state fluorescence measurements.[30] The same carotenoid-to-Bchl energy transfer efficiency was also observed from LH2-containing spheroidenone [Polivka, unpublished results].

Conclusions

The carotenoid in the reaction center absorbs in wavelength regions where the absorption of other cofactors is weak. Therefore, the carotenoid extends the overall absorption efficiency of the reaction center. However, the intact photosynthetic system contains a large number of antenna complexes that include carotenoid molecules whose absorption intensity is much higher at all wavelengths than that contributed by the reaction center itself. Therefore, the contribution of the reaction center carotenoid to overall light harvesting efficiency is presumably very small. What is clear from this study and previous work[30] is that the carotenoid in the reaction center can

carry out efficient singlet excitation energy transfer to Bchl once it is excited, suggesting a moderate coupling between the S_1 excited singlet states of the carotenoid and the bacteriochlorophylls in the reaction center. Apparently the fact that a 15-*cis*-carotenoid is present in the bacterial reaction center, when most antenna carotenoid molecules are all-trans, is not a key factor in determining the ability of the carotenoid to play a role in singlet energy transfer.

Acknowledgment. This work was supported by the National Science Foundation (MCB-0131776). This is publication #581 from the Center for the Study of Early Events in Photosynthesis, Arizona State University.

References and Notes

(1) Koyama, Y.; Kuki, M.; Andersson, P. O.; Gillbro, T. *Photochem. Photobiol.* **1996**, *63*, 243−256.

(2) Frank, H. A.; Farhoosh, R.; Gebhard, R.; Lugtenburg, J.; Gosztola, D.; Wasielewski, M. R. *Chem. Phys. Lett.* **1993**, *207*, 88−92.

(3) Frank, H. A.; Cogdell, R. J. In *Carotenoids in Photosynthesis*; Young, A. J., Britton G, Eds.; Chapman & Hall: London, UK, 1993; pp 252−326.

(4) Parson, W. W.; Monger, T. G. *Brookhaven Symp.* **1976**, *Biol 28*, 195−212.

(5) Schenck, C. C.; Mathis, P.; Lutz, M. *Photochem. Photobiol.* **1984**, *39*, 407−417.

(6) Takiff, L.; Boxer, S. G. *Biochim. Biophys. Acta* **1988**, *932*, 325−334.

(7) Lous, E. K.; Hoff, A. J. *Biochim. Biophys. Acta* **1989**, *974*, 88−103.

(8) Jordan, P.; Fromme, P.; Witt, H.-T.; Klukas, O.; Saenger, W.; Krauss, N. *Nature* **2001**, *411*, 909−917.

(9) Macpherson, A. N.; Gillbro, T. *J. Phys. Chem. A* **1998**, *102*, 1089−5639.

(10) Akimoto, S.; Takaichi, S.; Ogata, T.; Nishimura, Y.; Yamazaki, I.; Mimuro, M. *Chem. Phys. Lett.* **1996**, *260*, 147−152.

(11) Krueger, B. P.; Scholes, G. D.; Jimenez, R.; Fleming, G. R. *J. Phys. Chem. B* **1998**, *102*, 2284−2292.

(12) Zhang, J.-P.; Fujii, R.; Qian, P.; Inaba, T.; Mizoguchi, T.; Koyama, Y.; Onaka, K.; Watanabe, Y.; Nagae, H. *J. Phys. Chem.* **2000**, *104*, 3683−3691.

(13) Macpherson, A. N.; Arellano, J. B.; Fraser, N. J.; Cogdell, R. J.; Gillbro, T. *Biophys. J.* **2001**, *80*, 923−930.

(14) Gradinaru, C. C.; van Stokkum, I. H. M.; Pascal, A. A.; van Grondelle, R.; van Amerongen, H. *J. Phys. Chem. B* **2000**, *104*, 9330−9342.

(15) Kennis, J. T. M.; Gobets, B.; van Stokkum, I. H. M.; Dekker: J. P.; van Grondelle, R.; Fleming, G. R. *J. Phys. Chem. B* **2001**, *105*, 4485−4494.

(16) Croce, R.; Müller, M. G.; Bassi, R.; Holzwarth, A. R. *Biophys. J.* **2001**, *80*, 901−915.

(17) Gradinaru, C. C.; Kennis, J. T. M.; Papagiannakis, E.; van Stokkum, I. H. M.; Cogdell, R. J.; Fleming, G. R.; Niederman, R. A.; van Grondelle, R. *Proc. Natl. Acad. Sci. U.S.A.* **2001**, *98*, 2364−2369.

(18) Polívka, T.; Herek, J. L.; Zigmantas, D.; Åkerlund, H.-E.; Sundström, V. *Proc. Natl. Acad. Sci. U.S.A.* **1999**, *96*, 4914−4917.

(19) Walla, P. J.; Linden, P. A.; Hsu, C.-P.; Scholes, G. D.; Fleming, G. R. *Proc. Natl. Acad. Sci. U.S.A.* **2000**, *97*, 10808−10813.

(20) Cerullo, G.; Polli, D.; Lanzani, G.; de Silvestri, S.; Hashimoto, H.; Cogdell, R. J. *Science* **2002**, *298*, 2395−2398.

(21) Wasielewski, M. R.; Kispert, L. D. *Chem. Phys. Lett.* **1986**, *128*, 238−243.

(22) Frank, H. A.; Cogdell, R. J. *Photochem. Photobiol.* **1996**, *63*, 257−264.

(23) Goldsmith, J. O.; Boxer, S. G. *Biochim. Biophys. Acta* **1996**, *1276*, 171−175.

(24) Bautista, J. A.; Chynwat, V.; Cua, A.; Jansen, F. J.; Lugtenburg, J.; Gosztola, D.; Wasielewski, M. R.; Frank, H. A. *Photosyn. Res.* **1998**, *55*, 49−65.

(25) McAuley, K. E.; Fyfe, P. K.; Ridge, J. P.; Cogdell, R. J.; Isaacs, N. W.; Jones, M. R. *Biochemistry* **2000**, *39*, 15032−15043.

(26) Allen, J. P.; Feher, G.; Yeates, T. O.; Komiya, H.; Rees, D. C. *Proc. Natl. Acad. Sci. U.S.A.* **1987**, *84*, 5730−5734.

(27) Boucher, F.; Gingras, G. *Photochem. Photobiol.* **1984**, *40*, 277−281.

(28) Koyama, Y. In *Photosynthesis*: *From Light to Biosphere*; Mathis, P., Ed.; Kluwer Academic Publishers: Dordrecht, The Netherlans, 1995; Vol. 4, pp 83−86.

(29) Frank, H. A.; Violette, C. A. *Biochim. Biophys. Acta* **1989**, *976*, 222−232.

(30) Cogdell, R. J.; Parson, W. W.; Kerr, M. *Biochim. Biophys. Acta* **1976**, *430*, 83−93.

(31) Katilius, E.; Turanchik, T.; Lin, S.; Taguchi, A. K. W.; Woodbury, N. W. *J. Phys. Chem. B* **1999**, *103*, 7386−7389.

(32) Freiberg, A.; Timpmann, K.; Lin, S.; Woodbury, N. W. *J. Phys. Chem. B* **1998**, *102*, 10974−10982.

(33) Zhang, J.-P.; Inaba, T.; Watanabe, Y.; Koyama, Y. *Chem. Phys. Lett.* **2000**, *331*, 154−162.

(34) Walla, P. J.; Linden, P. A.; Ohta, K.; Fleming, G. R. *J. Phys. Chem. A* **2002**, *106*, 1909−1916.

(35) de Weerd, F. L.; van Stokkum, I. H. M.; van Grondelle, R. *Chem. Phys. Lett.* **2002**, *354*, 38−43.

(36) Walla, P. J.; Yom, J.; Krueger, B. P.; Fleming, G. R. *J. Phys. Chem. B* **2000**, *104*, 4799−4806.

(37) Kirmaier, C.; Holten, D. *Photosynth. Res.* **1987**, *13*, 225−260.

(38) Frank, H. A.; Bautista, J. A.; Josue, J.; Pendon, Z.; Hiller, R. G.; Sharples, F. P.; Gosztola, D.; Wasielewski, M. R. *J. Phys. Chem. B* **2000**, *104*, 4569−4577.

(39) Angerhofer, A.; Bornhäuser, F.; Aust, V.; Hartwichd, G.; Scheer, H. *Biochim. Biophys. Acta* **1998**, *1356*, 404−420.

(40) Holten, D.; Windsor, M. W.; Parson, W. W.; Thornber, J. P. *Biochim. Biophys. Acta* **1978**, *501*, 112−126.

(41) Breton, J.; Martin, J.-L.; Migus, A.; Antonetti, A.; Orszag, A. In *Ultrafast Phenomena V*; Proceedings of the 5th OSA Topical Meeting, Snowmass, CO, June 16−19, 1986; Fleming, G. R., Siegman, A.E., Eds.; Springer-Verlag: New York, 1986.

(42) Jia, Y.; Jonas, D. M.; Joo, T.; Nagasawa, Y.; Lang, M. J.; Fleming, G. R. *J. Phys. Chem.* **1995**, *99*, 6263−6266.

(43) Stanley, R. J.; King, B.; Boxer, S. G. *J. Phys. Chem.* **1996**, *100*, 12052−12059.

(44) Lin, S.; Taguchi, A. K. W.; Woodbury, N. W. *J. Phys. Chem.* **1996**, *100*, 17067−17078.

(45) deWinter, A.; Boxer, S. G. *J. Phys. Chem. B* **1999**, *103*, 8786−8789.

(46) Hsu, C.-P.; Walla, P. J.; Head-Gordon, M.; Fleming, G. R. *J. Phys. Chem.* **2001**, *105*, 11016−11025.

(47) Ritz, T.; Damjanovic, A.; Schulten, K.; Zhang, J.-P.; Koyama, Y. *Photosynth. Res.* **2000**, *66*, 125−144.

(48) de Weerd, F. L.; Kennis, J. T. M.; Dekker: J. P.; van Grondelle, R. *J. Phys. Chem. B* **2003**, *107*, 5995−6002.

(49) Bondarev, S. L.; Tikhomirov, S. A.; Bachilo, S. M. *SPIE* **1990**, *1403*, 497−499.

(50) Polívka, T.; Zigmantas, D.; Herek, J. L.; He, Z.; Pascher, T.; Pullerits, T.; Cogdell, R. J.; Frank, H. A.; Sundström, V. *J. Phys. Chem. B* **2002**, *106*, 11016−11025.